

Supporting Information

Modulation of the magnetic properties of mononuclear Dy(III) complexes by tuning the coordination geometry and local symmetry

Xuejuan Zhou,^{a#} Huiliang Qin,^{a#} Zhaopeng Zeng,^{b#} Shuchang Luo,^{*d} Tao Yang,^c Peipei Cen,^{*a} Xiangyu Liu^{*b}

^aCollege of Public Health, Key Laboratory of Environmental Factors and Chronic Disease Control, Ningxia Medical University, Yinchuan 750021, China.

^bState Key Laboratory of High-Efficiency Utilization of Coal and Green Chemical Engineering, College of Chemistry and Chemical Engineering, School of Civiland Hydraulic Engineering, Ningxia University, Yinchuan 750021, China.

^cNingxia People's Hospital, Yinchuan 753009, China.

^dCollege of Chemical Engineering, Guizhou University of Engineering Science, Bijie 551700, China.

These authors contributed equally to this work.

*Corresponding author

Dr. Peipei Cen

E-mail address: 13895400691@163.com

Prof. Xiangyu Liu

E-mail: xiangyuliu432@126.com

Dr. Shuchang Luo

Email: luosc@gues.edu.cn

Contents

- Table S1.** Crystal data and structure refinement details for **1-3**.
- Table S2.** Selected bond lengths (\AA) and bond angles ($^\circ$) for **1-3**.
- Table S3.** Hydrogen-bonded parameters (\AA , $^\circ$) for **2**.
- Table S4.** Continuous Shape Measurements (CShMs) for Dy(III) ions in **1-3** by SHAPE 2.1.
- Table S5.** Relaxation fitting parameters from least-squares fitting of $\chi(f)$ data under 1000 Oe dc field of **1**.
- Table S6.** Relaxation fitting parameters from least-squares fitting of $\chi(f)$ data under 1000 Oe dc field of **2**.
- Table S7.** Relaxation fitting parameters from least-squares fitting of $\chi(f)$ data under 500 Oe dc field of **3**.
- Table S8.** Calculated energy levels (cm^{-1}) and g (g_x , g_y , g_z) tensors and τ_{QTM} (s) of the lowest eight Kramers doublets (KDs) of **1**, **1a**, **2a**, **2b** and **3** using CASSCF/RASSI-SO with ORCA.
- Table S9.** Wave functions with definite projection of the total moment $| m_j \rangle$ for the lowest eight KDs of **1**, **1a**, **2a**, **2b** and **3** using CASSCF/RASSI-SO with ORCA.
- Table S10.** Mulliken atomic charge on the metal atoms and donor atoms in the ground state of **1**, **1a**, **2a**, **2b** and **3** calculated within B3LYP-D3/DKH-def2-TZVP level.
- Table S11.** Mulliken spin density of **1**, **1a**, **2a**, **2b** and **3**.
- Table S12.** Calculated crystal field parameters B (k , q) for **1**, **1a**, **2a**, **2b** and **3** using CASSCF/RASSI-SO with ORCA.
- Fig. S1** Crystal packing diagram for complex **1**. All hydrogen atoms, solvent molecules, and the counter ion $[\text{BPh}_4]^+$ for **1** are omitted for clarity.
- Fig. S2** (a) Crystal packing diagram for complex **2**. All hydrogen atoms (except for the H atoms in the H-bonds), solvent molecules, and the counter ion $[\text{PF}_6]^+$ for **2** are omitted for clarity. (b) Hydrogen bonding in complex **2** (the dashed line represents the interaction).
- Fig. S3** Crystal packing diagram for complex **3**. All hydrogen atoms, solvent molecules, and the counter ion $[\text{BPh}_4]^+$ for **3** are omitted for clarity.
- Fig. S4** PXRD curves of **1** (a), **2** (b) and **3** (c).
- Fig. S5** M vs H/T curves for **1** (a), **2** (b) and **3** (c) at indicated temperatures.
- Fig. S6** Ac magnetic susceptibility measurements for **1** (a), **2** (b) and **3** (c) in zero static field.
- Fig. S7** Frequency dependence of χ''_M susceptibilities for **1** (a), **2** (b) and **3** (c) under different dc fields.
- Fig. S8** Temperature dependence of the in-phase (χ'_M , top) and out-of-phase (χ''_M , bottom) ac susceptibilities at different frequencies under the external dc fields for complexes **1** (a, d), **2** (b, e) and **3** (c, f).
- Fig. S9** Frequency dependence of χ'_M susceptibilities for **1** (a), **2** (b) and **3** (c) under the external dc fields.
- Fig. S10** Frequency dependence of χ''_M susceptibilities for **1** under the external dc fields.
- Fig. S11** Cole-Cole plots under the static dc fields for **1** (a), **2** (b) and **3** (c). The solid lines represent the best fit to the measured results.
- Fig. S12** Calculated orientations of the local main magnetic axes on Dy(III) in the ground KDs of **1** (a), **1a** (b), **2a** (c), **2b** (d) and **3** (e).
- Fig. S13** Predicted effective barrier and relaxation contributions from various KDs of complexes **1** (a), **1a** (b), **2a** (c), **2b** (d) and **3** (e), U_{eff} is represented as a dashed black line, and its value is indicated on the right y-axis, the left y-axis represents the relative contribution of each KD to relaxation.

Table S1. Crystal data and structure refinement details for **1-3**.

complex	1	2	3
Empirical formula	C ₅₁ H ₅₄ BCl ₂ DyN ₆ O ₄	C ₆₈ H ₆₉ Cl ₈ Dy ₂ F ₁₂ N ₁₆ O ₁₇ P ₂	C ₆₀ H ₅₄ BCl ₈ DyN ₈ O ₆
Formula weight	1059.23	2280.93	1440.02
Temperature	296.0 K	150.0 K	296.0 K
Crystal system	triclinic	triclinic	monoclinic
Space group	<i>P</i> $\bar{1}$	<i>P</i> $\bar{1}$	<i>P</i> 2 ₁ / <i>n</i>
<i>a</i> (Å)	10.4067(5)	12.6622(7)	12.429(5)
<i>b</i> (Å)	14.5674(7)	18.6466(12)	16.344(6)
<i>c</i> (Å)	16.9951(9)	19.8147(13)	30.943(10)
α (°)	75.868(2)	105.480(2)	90
β (°)	81.870(2)	91.339(2)	93.964(12)
γ (°)	79.324(2)	103.205(2)	90
<i>V</i> (Å ³)	2442.7(2)	4371.7(5)	6271(4)
<i>Z</i>	2	2	4
<i>D</i> (g/cm ³)	1.418	1.733	1.525
<i>Mu</i> (mm ⁻¹)	1.614	2.075	1.589
<i>F</i> (0 0 0)	1063.0	2262.0	2900.0
Completeness	99.7	99.3	98.8
Unique reflections lections	11235	14798	14346
Observed reflections	61817	68773	132829
<i>R</i> _{int}	0.0540	0.0441	0.0355
Final <i>R</i> indices [<i>I</i> > 2σ(<i>I</i>)]	<i>R</i> ₁ = 0.0348 <i>wR</i> ₂ = 0.0700	<i>R</i> ₁ = 0.0398 <i>wR</i> ₂ = 0.0988	<i>R</i> ₁ = 0.0417 <i>wR</i> ₂ = 0.1101
<i>R</i> indices (all data)	<i>R</i> ₁ = 0.0475 <i>wR</i> ₂ = 0.0749	<i>R</i> ₁ = 0.0507 <i>wR</i> ₂ = 0.1056	<i>R</i> ₁ = 0.0467 <i>wR</i> ₂ = 0.1131
Goodness-of-fit on <i>F</i> ²	1.060	1.078	1.131

Table S2. Selected bond lengths (\AA) and bond angles ($^\circ$) for **1-3**.

Complex 1			
Dy(1)-N(1)	2.678(2)	N(5)-Dy(1)-N(3)	120.35(9)
Dy(1)-N(2)	2.588(2)	N(5)-Dy(1)-N(4)	60.37(8)
Dy(1)-N(3)	2.610(3)	N(5)-Dy(1)-N(6)	64.97(9)
Dy(1)-N(4)	2.669(2)	N(6)-Dy(1)-N(1)	59.47(8)
Dy(1)-N(5)	2.587(3)	N(6)-Dy(1)-N(4)	118.92(8)
Dy(1)-N(6)	2.619(3)	O(1)-Dy(1)-N(1)	103.36(8)
Dy(1)-O(1)	2.495(2)	O(1)-Dy(1)-N(2)	128.24(8)
Dy(1)-O(2)	2.424(3)	O(1)-Dy(1)-N(3)	89.40(9)
Dy(1)-O(3)	2.426(2)	O(1)-Dy(1)-N(4)	69.03(8)
Dy(1)-O(4)	2.392(2)	O(1)-Dy(1)-N(5)	73.91(9)
N(2)-Dy(1)-N(1)	59.94(8)	O(1)-Dy(1)-N(6)	71.71(9)
N(2)-Dy(1)-N(3)	64.76(8)	O(2)-Dy(1)-N(1)	68.59(9)
N(2)-Dy(1)-N(4)	121.81(8)	O(2)-Dy(1)-N(2)	77.11(9)
N(2)-Dy(1)-N(6)	119.16(8)	O(2)-Dy(1)-N(3)	73.89(10)
N(3)-Dy(1)-N(1)	117.93(8)	O(2)-Dy(1)-N(4)	103.53(9)
N(3)-Dy(1)-N(4)	60.16(8)	O(2)-Dy(1)-N(5)	124.90(9)
N(3)-Dy(1)-N(6)	158.56(10)	O(2)-Dy(1)-N(6)	86.25(10)
N(4)-Dy(1)-N(1)	171.75(8)	O(2)-Dy(1)-O(1)	52.13(8)
N(5)-Dy(1)-N(1)	121.58(8)	O(2)-Dy(1)-O(3)	146.02(10)
N(5)-Dy(1)-N(2)	157.80(9)	O(3)-Dy(1)-N(1)	116.39(8)
O(3)-Dy(1)-N(2)	77.81(9)	O(4)-Dy(1)-N(2)	83.58(8)
O(3)-Dy(1)-N(3)	74.85(9)	O(4)-Dy(1)-N(3)	124.50(9)
O(3)-Dy(1)-N(4)	71.41(8)	O(4)-Dy(1)-N(4)	112.95(8)
O(3)-Dy(1)-N(5)	82.87(9)	O(4)-Dy(1)-N(5)	76.18(9)
O(3)-Dy(1)-N(6)	126.26(9)	O(4)-Dy(1)-N(6)	76.53(9)
O(3)-Dy(1)-O(1)	140.17(8)	O(4)-Dy(1)-O(1)	143.21(8)
O(4)-Dy(1)-N(1)	74.97(8)	O(4)-Dy(1)-O(2)	143.52(9)
N(3)-Dy(1)-C(30)	81.31(11)	O(4)-Dy(1)-O(3)	53.77(8)

Complex 2			
Dy(1)-N(1)	2.564(4)	Dy(2)-N(8)	2.613(4)
Dy(1)-N(2)	2.498(4)	Dy(2)-N(9)	2.625(4)
Dy(1)-N(3)	2.610(4)	Dy(2)-N(10)	2.501(4)
Dy(1)-N(4)	2.591(4)	Dy(2)-N(11)	2.574(5)
Dy(1)-N(5)	2.521(4)	Dy(2)-N(12)	2.598(5)
Dy(1)-N(6)	2.576(4)	Dy(2)-N(13)	2.529(5)
Dy(1)-O(1)	2.215(4)	Dy(2)-O(6)	2.221(3)
Dy(1)-O(4)	2.423(4)	Dy(2)-O(9)	2.364(4)
Dy(1)-O(5)	2.378(4)	Dy(2)-O(10)	2.478(4)
N(1)-Dy(1)-N(3)	113.14(15)	N(2)-Dy(1)-N(4)	122.66(15)
N(1)-Dy(1)-N(4)	143.97(14)	N(2)-Dy(1)-N(5)	164.35(15)
N(1)-Dy(1)-N(6)	61.50(15)	N(2)-Dy(1)-N(6)	121.55(15)

N(2)-Dy(1)-N(1)	62.48(16)	N(4)-Dy(1)-N(3)	60.03(14)
N(2)-Dy(1)-N(3)	62.65(15)	N(5)-Dy(1)-N(1)	124.37(15)
N(5)-Dy(1)-N(3)	118.89(14)	N(5)-Dy(1)-N(4)	61.67(13)
N(5)-Dy(1)-N(6)	62.88(14)	N(6)-Dy(1)-N(3)	160.56(15)
N(6)-Dy(1)-N(4)	112.06(13)	O(1)-Dy(1)-N(1)	69.89(14)
O(1)-Dy(1)-N(2)	92.08(15)	O(1)-Dy(1)-N(3)	77.00(16)
O(1)-Dy(1)-N(4)	74.21(15)	O(1)-Dy(1)-N(5)	103.49(14)
O(1)-Dy(1)-N(6)	83.77(15)	O(1)-Dy(1)-O(4)	142.97(15)
O(1)-Dy(1)-O(5)	146.13(15)	O(4)-Dy(1)-N(1)	74.06(14)
O(4)-Dy(1)-N(2)	78.43(14)	O(4)-Dy(1)-N(3)	126.34(15)
O(4)-Dy(1)-N(4)	140.52(14)	O(4)-Dy(1)-N(5)	89.83(14)
O(4)-Dy(1)-N(6)	71.75(13)	O(5)-Dy(1)-N(1)	136.65(14)
O(5)-Dy(1)-N(2)	87.12(15)	O(5)-Dy(1)-N(3)	72.62(15)
O(5)-Dy(1)-N(4)	77.84(14)	O(5)-Dy(1)-N(5)	79.06(14)
O(5)-Dy(1)-N(6)	124.93(14)	O(5)-Dy(1)-O(4)	69.83(14)
N(8)-Dy(2)-N(9)	60.34(13)	N(10)-Dy(2)-N(8)	123.47(14)
N(10)-Dy(2)-N(9)	63.13(13)	N(10)-Dy(2)-N(11)	62.39(14)
N(10)-Dy(2)-N(12)	121.02(15)	N(10)-Dy(2)-N(13)	162.74(15)
N(11)-Dy(2)-N(8)	145.96(13)	N(11)-Dy(2)-N(9)	113.91(13)
N(11)-Dy(2)-N(12)	61.51(15)	N(12)-Dy(2)-N(8)	112.89(14)
N(12)-Dy(2)-N(9)	162.51(14)	N(13)-Dy(2)-N(8)	61.01(15)
N(13)-Dy(2)-N(9)	118.39(15)	N(13)-Dy(2)-N(11)	124.87(15)
N(13)-Dy(2)-N(12)	63.36(16)	O(6)-Dy(2)-N(8)	74.07(14)
O(6)-Dy(2)-N(9)	80.67(13)	O(6)-Dy(2)-N(10)	97.07(14)
O(6)-Dy(2)-N(11)	71.89(13)	O(6)-Dy(2)-N(12)	81.92(14)
O(6)-Dy(2)-N(13)	100.14(14)	O(6)-Dy(2)-O(9)	151.01(14)
O(6)-Dy(2)-O(10)	141.35(15)	O(9)-Dy(2)-N(8)	81.38(14)
O(9)-Dy(2)-N(9)	73.81(14)	O(9)-Dy(2)-N(10)	83.64(14)
O(9)-Dy(2)-N(11)	131.33(14)	O(9)-Dy(2)-N(12)	122.56(15)
O(9)-Dy(2)-N(13)	80.65(15)	O(9)-Dy(2)-O(10)	67.05(15)
O(10)-Dy(2)-N(8)	141.54(15)	O(10)-Dy(2)-N(9)	125.31(14)
O(10)-Dy(2)-N(10)	75.69(14)	O(10)-Dy(2)-N(11)	71.23(14)
O(10)-Dy(2)-N(12)	70.68(15)	O(10)-Dy(2)-N(13)	91.55(15)

Complex 3			
Dy(1)-O(1)	2.223(3)	N(4)-Dy(1)-N(3)	61.49(11)
Dy(1)-O(4)	2.166(3)	N(4)-Dy(1)-N(5)	64.19(13)
Dy(1)-N(8)	2.580(3)	N(4)-Dy(1)-N(7)	117.56(11)
Dy(1)-N(3)	2.578(3)	N(5)-Dy(1)-N(8)	61.35(12)
Dy(1)-N(4)	2.537(3)	N(5)-Dy(1)-N(3)	117.18(11)
Dy(1)-N(5)	2.575(4)	N(5)-Dy(1)-N(7)	171.04(11)
Dy(1)-N(6)	2.518(3)	N(6)-Dy(1)-N(8)	61.68(12)
Dy(1)-N(7)	2.637(3)	N(6)-Dy(1)-N(7)	62.70(10)

O(1)-Dy(1)-N(8)	74.02(10)	N(6)-Dy(1)-N(3)	122.94(11)
O(1)-Dy(1)-N(3)	76.91(9)	N(6)-Dy(1)-N(4)	160.04(11)
O(1)-Dy(1)-N(4)	100.51(11)	N(6)-Dy(1)-N(5)	119.04(12)
O(1)-Dy(1)-N(5)	84.38(11)	O(4)-Dy(1)-N(5)	90.10(12)
O(1)-Dy(1)-N(6)	99.43(11)	O(4)-Dy(1)-N(6)	80.23(11)
O(1)-Dy(1)-N(7)	86.66(9)	O(4)-Dy(1)-N(7)	98.85(11)
O(4)-Dy(1)-O(1)	173.49(11)	N(8)-Dy(1)-N(7)	116.13(10)
O(4)-Dy(1)-N(8)	100.30(11)	N(3)-Dy(1)-N(8)	150.90(9)
O(4)-Dy(1)-N(3)	108.80(11)	N(3)-Dy(1)-N(7)	60.25(9)
O(4)-Dy(1)-N(4)	80.07(11)	N(4)-Dy(1)-N(8)	125.54(12)

Table S3. Hydrogen-bonded parameters (\AA , $^\circ$) for **2**.

Complex	D-H...A	d(D-H)	d(H...A)	d(D...A)	$\angle(\text{DHA})$
2	O4-H4A...O14 ¹	0.88	2.02	2.887(7)	173.0
	O4-H4B...O11	0.88	1.88	2.732(6)	163.7
	O5-H5D...O11	0.90	1.83	2.680(7)	157.3
	O5-H5E...O14A	0.90	1.94	2.753(9)	150.2
	O9-H9A...O13 ²	0.91	1.79	2.605(6)	148.3
	O9-H9B...O16 ²	0.91	2.02	2.836(8)	149.8
	O11-H11A...O13	0.87	1.86	2.721(7)	172.9
	O11-H11B...O16	0.87	2.05	2.876(9)	157.7

¹-1+X,+Y,+Z; ²+X,1+Y,+Z

Table S4. Continuous Shape Measurements (CShMs) for Dy(III) ions in **1-3** by SHAPE 2.1.

Configuration	ABOXIY, 1	Configuration	ABOXIY, 2	Configuration	ABOXIY, 3	
TD-10	2.109	MFF-9	3.472	3.922	HBPY-8	2.967
OBPY-10	15.997	HBPY-9	15.015	14.197	CU-8	11.348
PPR-10	11.076	JTC-9	13.524	14.078	SAPR-8	15.328
PAPR-10	11.438	JCCU-9	6.264	6.119	TDD-8	13.946
JBCCU-10	8.742	CCU-9	5.250	5.093	JGBF-8	4.301
JBCSAPR-10	3.927	JCSAPR-9	6.178	6.526	JETBPY-8	22.513
JMBIC-10	6.804	CSAPR-9	4.957	5.288	JBTPR-8	14.115
JATDI-10	18.459	JTCTPR-9	5.828	6.452	BTPR-8	13.933
JSPC-10	2.550	TCTPR-9	6.093	6.301	JSD-8	13.437
SDD-10	2.671	JTDIC-9	11.462	11.813	TT-8	11.954
HD-10	6.366	HH-9	4.051	3.697	ETBPY-8	19.926

Table S5. Relaxation fitting parameters from least-squares fitting of $\chi(f)$ data under 1000 Oe dc field of **1**.

$T(K)$	χ_T	χ_s	α
3	1.197	0.358	0.515
3.5	0.985	0.380	0.376
4	0.854	0.366	0.275
4.5	0.761	0.343	0.225
5	0.687	0.331	0.197
5.5	0.626	0.320	0.189
6	0.575	0.280	0.212
6.5	0.535	3.16×10^{-8}	0.322
7	0.497	5.03×10^{-8}	0.342
7.5	0.466	3.85×10^{-8}	0.438
8	0.438	7.44×10^{-8}	0.559

Table S6. Relaxation fitting parameters from least-squares fitting of $\chi(f)$ data under 1000 Oe dc field of **2**.

$T(K)$	χ_T	χ_s	α
5	2.149	0.957	0.367
5.5	1.949	0.923	0.329
6	1.787	0.870	0.308
6.5	1.650	0.814	0.293
7	1.531	0.709	0.319
8	1.342	0.652	0.284
9	1.197	0.538	0.281
10	1.071	0.388	0.262

Table S7. Relaxation fitting parameters from least-squares fitting of $\chi(f)$ data under 500 Oe dc field of **3**.

$T(K)$	χ_T	χ_s	α
2	2.613	0.106	0.309
2.5	2.151	0.090	0.217
3	1.841	0.074	0.169
3.5	1.598	0.062	0.143
4	1.405	0.051	0.126
4.5	1.255	0.041	0.118
5	1.132	0.033	0.116
5.5	1.030	0.030	0.114
6	0.947	0.039	0.113
6.5	0.875	0.067	0.104

Table S8. Calculated energy levels (cm^{-1}) and g (g_x , g_y , g_z) tensors and τ_{QTM} (s) of the lowest eight Kramers doublets (KDs) of **1**, **1a**, **2a**, **2b** and **3** using CASSCF/RASSI-SO with ORCA.

	KDs	E/cm^{-1}	g_x	g_y	g_z	g_z Angle/ $^\circ$	$\tau_{\text{QTM}}/\text{s}$
1	KD ₀	0.000	0.0086	0.0300	19.8911	--	7.728×10^{-5}
	KD ₁	135.381	0.3403	0.4595	16.8836	101.00	1.846×10^{-7}
	KD ₂	172.720	1.1244	2.1609	11.8082	104.89	7.259×10^{-9}
	KD ₃	198.838	9.3681	6.6819	1.7220	87.79	3.139×10^{-10}
	KD ₄	249.730	1.9616	2.6386	14.4972	55.38	4.912×10^{-9}
	KD ₅	302.777	0.2839	2.2431	16.6458	89.59	1.174×10^{-8}
	KD ₆	334.879	0.0214	1.3888	12.7757	84.46	2.379×10^{-8}
	KD ₇	363.346	0.3024	3.9791	15.1564	87.99	3.516×10^{-9}
1a	KD ₀	0.000	0.0000	0.0000	19.9828	--	9.792×10^5
	KD ₁	452.728	0.0000	0.0000	17.0576	1.51	3.842×10^3
	KD ₂	773.849	0.0001	0.0001	14.3403	0.61	1.324
	KD ₃	1026.546	0.0027	0.0029	11.6860	3.31	2.616×10^{-3}
	KD ₄	1249.325	0.0332	0.0379	9.0535	7.34	1.274×10^{-5}
	KD ₅	1447.014	0.3208	0.3837	6.4078	9.92	9.177×10^{-8}
	KD ₆	1601.640	2.5461	3.0726	3.8224	27.72	1.240×10^{-9}
	KD ₇	1692.073	13.39237	7.6377	1.1692	2.14	2.324×10^{-10}
2a	KD ₀	0.000	0.0315	0.1340	19.4796	--	7.620×10^{-5}
	KD ₁	82.844	0.0745	0.2004	18.6284	63.77	1.456×10^{-6}
	KD ₂	132.402	0.2838	0.9402	16.9403	132.41	6.284×10^{-8}
	KD ₃	170.564	1.5215	1.9508	16.4952	98.86	9.735×10^{-9}
	KD ₄	225.652	1.5268	2.0777	14.9452	37.88	8.150×10^{-9}
	KD ₅	258.999	4.6775	6.0662	8.5471	122.22	6.988×10^{-10}
	KD ₆	332.885	0.9674	1.0154	17.3019	115.89	3.153×10^{-8}
	KD ₇	395.283	0.1497	0.1774	18.9796	113.62	1.258×10^{-6}
2b	KD ₀	0.000	0.1316	0.1398	19.5184	--	1.892×10^{-6}
	KD ₁	92.678	0.1860	0.2914	19.1371	121.10	5.721×10^{-7}
	KD ₂	162.085	1.2929	2.8965	14.9207	41.31	5.416×10^{-9}
	KD ₃	193.599	0.9151	3.2440	15.4659	103.21	4.977×10^{-9}
	KD ₄	236.840	1.4818	4.8019	11.1230	135.31	1.727×10^{-9}
	KD ₅	296.235	1.9574	5.2631	9.7676	84.52	1.276×10^{-9}
	KD ₆	355.129	1.5686	2.7542	15.9311	57.95	5.776×10^{-9}
	KD ₇	453.361	0.1594	0.2672	19.1980	71.29	7.087×10^{-7}
3	KD ₀	0.000	0.0181	0.0280	19.9138	--	6.417×10^{-5}
	KD ₁	291.753	1.3189	2.2459	15.6436	2.01	8.352×10^{-9}
	KD ₂	416.542	1.0787	2.9242	13.8248	93.39	5.211×10^{-9}
	KD ₃	505.181	3.1951	4.2268	11.6370	82.12	1.627×10^{-9}

KD ₄	553.397	0.1087	1.8287	9.2537	93.11	1.004×10^{-8}
KD ₅	579.551	4.3609	5.2768	8.7172	109.40	8.449×10^{-10}
KD ₆	677.018	5.0112	5.1992	10.0056	92.32	8.453×10^{-10}
KD ₇	739.008	0.3545	1.0256	16.3616	77.66	4.957×10^{-8}

Table S9. Wave functions with definite projection of the total moment $|m_J\rangle$ for the lowest eight KDs of **1**, **1a**, **2a**, **2b** and **3** using CASSCF/RASSI-SO with ORCA.

	E/cm^{-1}	wave functions				
	0.000	99.4%	$ \pm 15/2\rangle$			
	135.381	6.4%	$ \pm 13/2\rangle + 20.9\% \pm 9/2\rangle + 32.2\% \pm 7/2\rangle + 25.7\% \pm 5/2\rangle + 10.5\% \pm 3/2\rangle$			
	172.720	26.1%	$ \pm 13/2\rangle + 24.4\% \pm 11/2\rangle + 18.7\% \pm 9/2\rangle + 10.8\% \pm 7/2\rangle + 4.2\% \pm 5/2\rangle + 5.1\% \pm 3/2\rangle + 10.8\%$			
1	198.838	49.0%	$ \pm 13/2\rangle + 6.4\% \pm 11/2\rangle + 22.6\% \pm 9/2\rangle + 11.9\% \pm 7/2\rangle + 4.9\% \pm 5/2\rangle + 4.1\% \pm 3/2\rangle$			
	249.730	17.9%	$ \pm 13/2\rangle + 45.1\% \pm 11/2\rangle + 12.6\% \pm 9/2\rangle + 6.4\% \pm 7/2\rangle + 5.7\% \pm 5/2\rangle + 5.4\% \pm 3/2\rangle + 6.7\% \pm 1/2\rangle$			
	302.777	23.3%	$ \pm 7/2\rangle + 43.6\% \pm 5/2\rangle + 22.2\% \pm 3/2\rangle + 7.0\% \pm 1/2\rangle$			
	334.879	3.0%	$ \pm 11/2\rangle + 18.0\% \pm 9/2\rangle + 13.8\% \pm 7/2\rangle + 10.3\% \pm 5/2\rangle + 35.5\% \pm 3/2\rangle + 18.6\% \pm 1/2\rangle$			
	363.346	3.6%	$ \pm 13/2\rangle + 13.3\% \pm 11/2\rangle + 5.1\% \pm 9/2\rangle + 5.7\% \pm 5/2\rangle + 16.9\% \pm 3/2\rangle + 53.8\% \pm 1/2\rangle$			
	0.000	100.0%	$ \pm 15/2\rangle$			
	452.728	99.8%	$ \pm 13/2\rangle$			
	773.849	99.5%	$ \pm 11/2\rangle$			
1a	1026.546	99.3%	$ \pm 9/2\rangle$			
	1249.325	99.0%	$ \pm 7/2\rangle$			
	1447.014	97.5%	$ \pm 5/2\rangle$			
	1601.640	94.0%	$ \pm 3/2\rangle + 4.4\% \pm 1/2\rangle$			
	1692.073	4.2%	$ \pm 3/2\rangle + 95.2\% \pm 1/2\rangle$			
	0.000	95.2%	$ \pm 15/2\rangle + 2.8\% \pm 9/2\rangle$			
	82.844	7.9%	$ \pm 11/2\rangle + 19.7\% \pm 9/2\rangle + 32.5\% \pm 7/2\rangle + 27.5\% \pm 5/2\rangle + 8.9\% \pm 3/2\rangle$			
	132.402	33.3%	$ \pm 13/2\rangle + 18.2\% \pm 11/2\rangle + 8.3\% \pm 9/2\rangle + 16.6\% \pm 7/2\rangle + 16.5\% \pm 5/2\rangle + 7.4\% \pm 3/2\rangle$			
	170.564	20.3%	$ \pm 11/2\rangle + 11.8\% \pm 7/2\rangle + 6.0\% \pm 5/2\rangle + 29.0\% \pm 3/2\rangle + 26.4\% \pm 1/2\rangle$			
	225.652	29.7%	$ \pm 13/2\rangle + 37.6\% \pm 11/2\rangle + 14.3\% \pm 5/2\rangle + 6.8\% \pm 3/2\rangle + 10.0\% \pm 1/2\rangle$			
2a	258.999	19.7%	$ \pm 13/2\rangle + 4.1\% \pm 11/2\rangle + 26.9\% \pm 9/2\rangle + 3.7\% \pm 7/2\rangle + 4.2\% \pm 5/2\rangle + 14.2\% \pm 3/2\rangle + 26.1\% \pm 1/2\rangle$			
	332.885	9.2%	$ \pm 13/2\rangle + 15.2\% \pm 11/2\rangle + 8.0\% \pm 9/2\rangle + 19.2\% \pm 7/2\rangle + 11.7\% \pm 5/2\rangle + 15.1\% \pm 3/2\rangle + 20.6\% \pm 1/2\rangle$			
	395.283	4.8%	$ \pm 13/2\rangle + 14.8\% \pm 11/2\rangle + 12.6\% \pm 9/2\rangle + 14.6\% \pm 7/2\rangle + 19.6\% \pm 5/2\rangle + 18.6\% \pm 3/2\rangle + 14.6\% \pm 1/2\rangle$			
	0.000	95.9%	$ \pm 15/2\rangle + 2.6\% \pm 7/2\rangle$			
2b	92.678	5.9%	$ \pm 13/2\rangle + 12.4\% \pm 11/2\rangle + 27.1\% \pm 9/2\rangle + 24.5\% \pm 7/2\rangle + 21.6\% \pm 5/2\rangle + 5.7\% \pm 3/2\rangle$			
	162.085	38.9%	$ \pm 13/2\rangle + 13.7\% \pm 11/2\rangle + 18.3\% \pm 7/2\rangle + 18.0\% \pm 5/2\rangle + 11.3\% \pm 3/2\rangle + 4.3\% \pm 1/2\rangle$			

		193.599	3.9% $\pm 13/2$ > + 8.4% $\pm 11/2$ > + 19.4% $\pm 9/2$ > + 11.1% $\pm 7/2$ > + 7.7% $\pm 5/2$ > + 29.9% $\pm 3/2$ > + 18.8% $\pm 1/2$ >
		236.840	20.8% $\pm 13/2$ > + 28.9% $\pm 11/2$ > + 3.4% $\pm 9/2$ > + 17.5% $\pm 5/2$ > + 23.3% $\pm 1/2$ >
		296.235	15.6% $\pm 13/2$ > + 24.9% $\pm 9/2$ > + 7.7% $\pm 7/2$ > + 8.8% $\pm 5/2$ > + 25.5% $\pm 3/2$ > + 15.1% $\pm 1/2$ >
		355.129	10.5% $\pm 13/2$ > + 23.4% $\pm 11/2$ > + 12.0% $\pm 9/2$ > + 19.0% $\pm 7/2$ > + 9.8% $\pm 5/2$ > + 6.0% $\pm 3/2$ > + 18.6% $\pm 1/2$ >
		453.361	4.4% $\pm 13/2$ > + 11.4% $\pm 11/2$ > + 10.0% $\pm 9/2$ > + 12.5% $\pm 7/2$ > + 18.4% $\pm 5/2$ > + 21.5% $\pm 3/2$ > + 21.4% $\pm 1/2$ >
		0.000	99.6% $\pm 15/2$ >
		291.753	90.3% $\pm 13/2$ > + 6.6% $\pm 1/2$ >
		416.542	7.8% $\pm 13/2$ > + 17.8% $\pm 11/2$ > + 3.0% $\pm 9/2$ > + 3.9% $\pm 7/2$ > + 6.3% $\pm 5/2$ > + 20.1% $\pm 3/2$ > + 40.9% $\pm 1/2$ >
3		505.181	21.7% $\pm 11/2$ > + 12.4% $\pm 9/2$ > + 3.0% $\pm 7/2$ > + 46.1% $\pm 3/2$ > + 14.8% $\pm 1/2$ >
		553.397	20.1% $\pm 11/2$ > + 15.1% $\pm 7/2$ > + 52.7% $\pm 5/2$ > + 8.3% $\pm 3/2$ >
		579.551	35.4% $\pm 11/2$ > + 6.4% $\pm 9/2$ > + 15.0% $\pm 7/2$ > + 6.2% $\pm 5/2$ > + 4.9% $\pm 3/2$ > + 31.3% $\pm 1/2$ >
		677.018	3.3% $\pm 11/2$ > + 58.4% $\pm 9/2$ > + 15.3% $\pm 7/2$ > + 5.7% $\pm 5/2$ > + 13.2% $\pm 3/2$ > + 3.6% $\pm 1/2$ >
		739.008	17.5% $\pm 9/2$ > + 47.4% $\pm 7/2$ > + 26.8% $\pm 5/2$ > + 6.5% $\pm 3/2$ >

Table S10. Mulliken atomic charge on the metal atoms and donor atoms in the ground state of **1**, **1a**, **2a**, **2b** and **3** calculated within B3LYP-D3/DKH-def2-TZVP level.

	1		1a		2a		2b		3
Dy	1.9499	Dy	1.7250	Dy1	1.7571	Dy2	1.6794	Dy	1.9386
N1	-0.2872	O1	-0.4669	N1	-0.4084	N8	-0.4347	N3	-0.3326
N2	-0.3082	O2	-0.4839	N2	-0.3905	N9	-0.3679	N4	-0.3268
N3	-0.2988	O3	-0.4715	N3	-0.3473	N10	-0.4024	N5	-0.2934
N4	-0.2933	O4	-0.4736	N4	-0.4276	N11	-0.3907	N6	-0.3175
N5	-0.3227			N5	-0.3893	N12	-0.4251	N7	-0.3092
N6	-0.3040			N6	-0.3321	N13	-0.3778	N8	-0.3055
O1	-0.4997			O1	-0.6430	O6	-0.6464	O1	-0.7185
O2	-0.5274			O4	-0.5217	O9	-0.5806	O4	-0.6931
O3	-0.5157			O5	-0.5787	O10	-0.5765		
O4	-0.5237								

Table S11. Mulliken spin density of **1**, **1a**, **2a**, **2b** and **3**.

	1	1a		2a		2b		3	
Atoms	Spin density	Atoms	Spin density	Atoms	Spin density	Atoms	Spin density	Atoms	Spin density
Dy	5.0218	Dy	4.9766	Dy	5.0178	Dy	5.0124	Dy	5.0022
N1	-0.0016	O1	0.0084	N1	-0.2816	N1	-0.2859	N1	-0.0031
N2	-0.0038	O2	0.0068	N2	-0.1506	N2	-0.0830	N2	-0.0024
N3	-0.0040	O3	-0.0023	N3	0.0966	N3	0.0970	N3	-0.0027
N4	-0.0018	O4	0.0135	N4	0.2717	N4	0.2922	N4	-0.0026
N5	-0.0039			N5	0.0981	N5	0.1067	N5	-0.0016
N6	-0.0033			N6	-0.0629	N6	-0.1266	N6	-0.0027
O7	-0.0034			O7	-0.0051	O7	-0.0019	O7	0.0024
O8	-0.0021			O8	0.0075	O8	-0.0061	O8	0.0011
O9	-0.0020			O9	0.0025	O9	0.0029		
O10	-0.0025								

Table S12. Calculated crystal field parameters $B(k, q)$ for **1**, **1a**, **2a**, **2b** and **3** using CASSCF/RASSI-SO with ORCA.

k	q	$B_{k,q}$				
		1	1a	2a	2b	3
2	-2	1.55	-1.65	-2.03	-1.37	-1.47×10^{-1}
2	-1	9.51×10^{-1}	4.48×10^{-2}	5.45	4.67	-1.71×10^{-1}
2	0	-3.21	-22.50	-2.01	-2.39	-2.87
2	1	3.61×10^{-1}	-1.88×10^{-1}	8.52×10^{-1}	5.67	-7.48×10^{-1}
2	2	5.25×10^{-2}	5.58×10^{-1}	8.91×10^{-1}	-3.14	1.24
4	-4	-8.09×10^{-3}	-3.17×10^{-3}	1.39×10^{-1}	-6.18×10^{-2}	-2.18×10^{-4}
4	-3	4.06×10^{-3}	2.62×10^{-3}	2.58×10^{-1}	-3.08×10^{-1}	-3.61×10^{-3}
4	-2	-2.37×10^{-4}	-2.31×10^{-2}	-4.34×10^{-2}	-1.01×10^{-1}	-1.35×10^{-3}
4	-1	-6.39×10^{-3}	-1.94×10^{-2}	-8.46×10^{-2}	-3.70×10^{-2}	3.43×10^{-3}
4	0	-1.76×10^{-2}	-4.06×10^{-3}	-2.39×10^{-2}	-2.48×10^{-2}	-1.18×10^{-2}
4	1	1.07×10^{-2}	3.95×10^{-2}	4.58×10^{-2}	-4.09×10^{-2}	5.01×10^{-3}
4	2	-7.82×10^{-3}	1.39×10^{-2}	8.29×10^{-2}	-1.26×10^{-2}	-3.02×10^{-4}
4	3	-3.47×10^{-3}	-2.82×10^{-2}	2.24×10^{-1}	3.48×10^{-2}	-7.83×10^{-4}
4	4	-3.32×10^{-2}	6.61×10^{-3}	-3.84×10^{-2}	1.61×10^{-1}	-8.45×10^{-3}
6	-6	1.45×10^{-2}	1.88×10^{-5}	4.30×10^{-3}	-4.37×10^{-3}	-7.29×10^{-4}
6	-5	-5.60×10^{-4}	-3.92×10^{-5}	-2.61×10^{-3}	-2.73×10^{-4}	-1.97×10^{-4}
6	-4	-4.73×10^{-4}	-1.64×10^{-4}	2.90×10^{-3}	-1.43×10^{-3}	-1.28×10^{-5}
6	-3	4.73×10^{-4}	-1.09×10^{-4}	5.26×10^{-3}	-8.78×10^{-3}	1.58×10^{-5}
6	-2	-1.73×10^{-3}	9.99×10^{-4}	2.19×10^{-3}	3.99×10^{-3}	-7.13×10^{-5}
6	-1	-4.76×10^{-3}	1.16×10^{-3}	9.98×10^{-3}	5.71×10^{-3}	-4.08×10^{-5}
6	0	-8.67×10^{-4}	-7.71×10^{-4}	-5.27×10^{-4}	-7.56×10^{-4}	2.99×10^{-5}
6	1	-7.66×10^{-4}	-2.23×10^{-3}	4.15×10^{-3}	5.69×10^{-3}	-1.31×10^{-6}
6	2	1.36×10^{-3}	-6.50×10^{-4}	-3.54×10^{-3}	1.83×10^{-3}	1.30×10^{-5}
6	3	9.06×10^{-4}	9.46×10^{-4}	9.26×10^{-3}	4.60×10^{-3}	-3.17×10^{-5}
6	4	1.67×10^{-3}	2.01×10^{-4}	-1.28×10^{-3}	4.46×10^{-3}	-8.05×10^{-5}

6	5	-7.76×10^{-3}	1.27×10^{-5}	1.37×10^{-3}	2.41×10^{-3}	-2.96×10^{-5}
6	6	-3.00×10^{-3}	1.09×10^{-5}	4.09×10^{-3}	-3.76×10^{-3}	1.06×10^{-4}

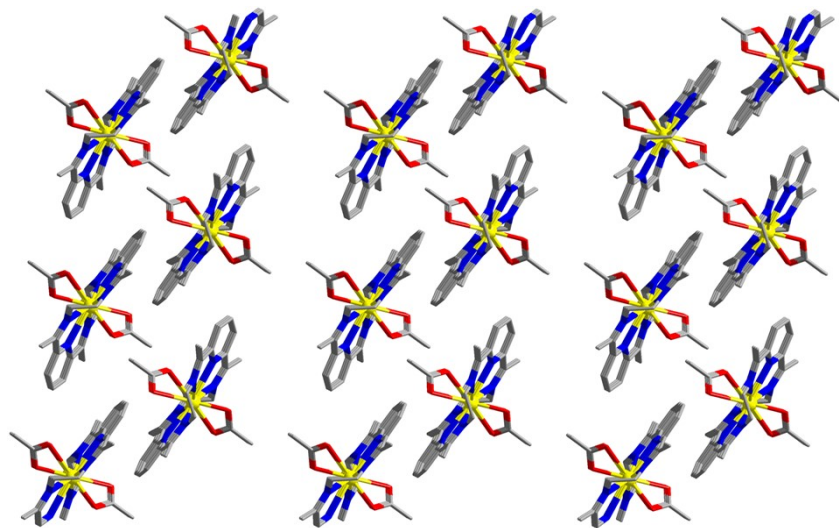


Fig. S1 Crystal packing diagram for complex **1**. All hydrogen atoms, solvent molecules, and the counter ion $[\text{BPh}_4]^+$ for **1** are omitted for clarity.

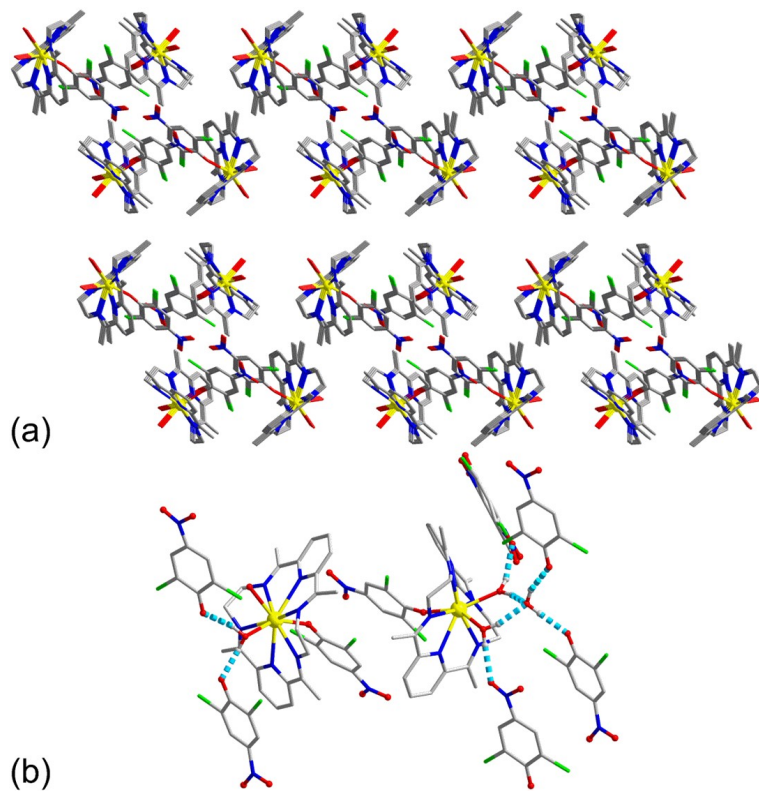


Fig. S2 (a) Crystal packing diagram for complex **2**. All hydrogen atoms (except for the H atoms in the H-bonds), solvent molecules, and the counter ion $[\text{PF}_6]^+$ for **2** are omitted for clarity. (b) Hydrogen bonding in complex **2** (the dashed line represents the interaction).

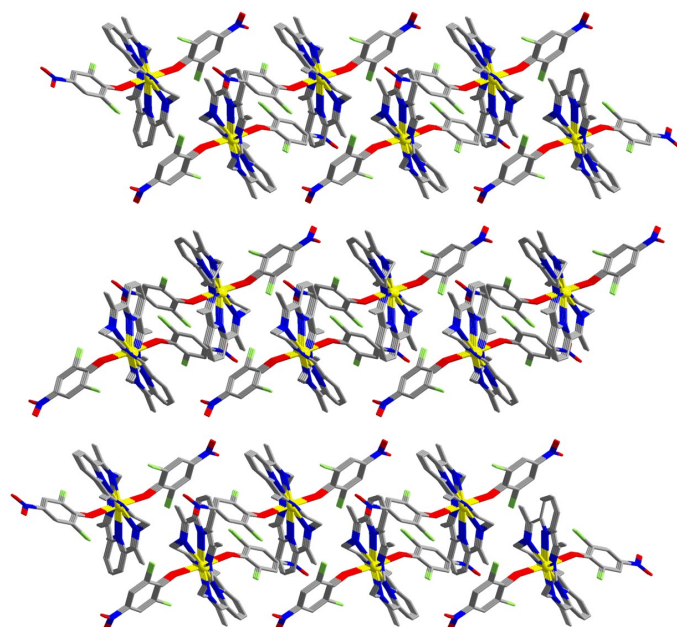


Fig. S3 Crystal packing diagram for complex **3**. All hydrogen atoms, solvent molecules, and the counter ion $[\text{BPh}_4]^+$ for **3** are omitted for clarity.

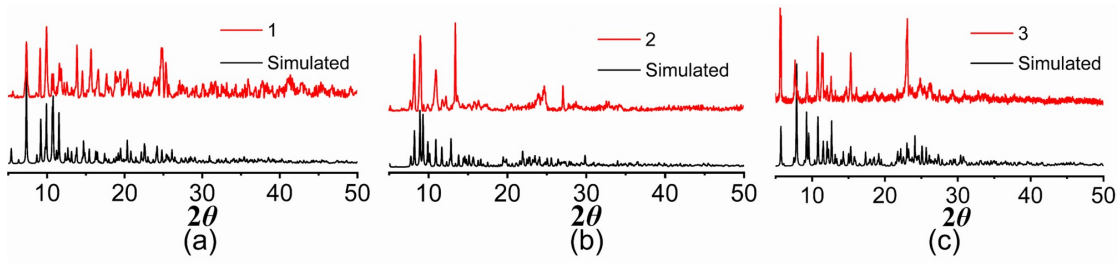


Fig. S4 PXRD curves of **1** (a), **2** (b) and **3** (c).

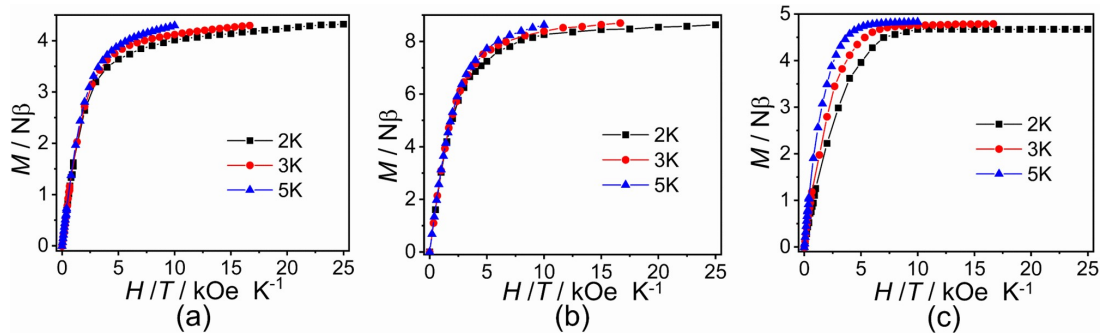


Fig. S5 M vs H/T curves for **1** (a), **2** (b) and **3** (c) at indicated temperatures.

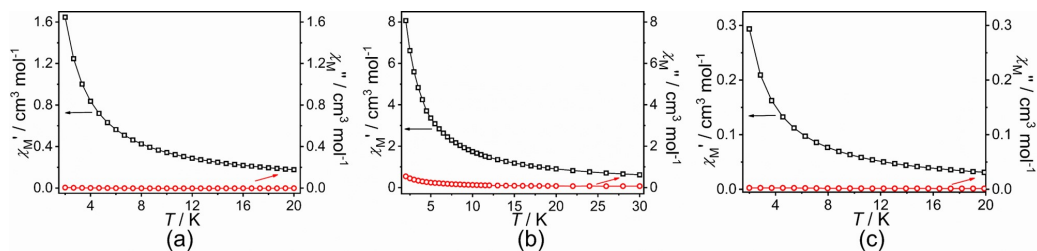


Fig. S6 Ac magnetic susceptibility measurements for **1** (a), **2** (b) and **3** (c) in zero static field.

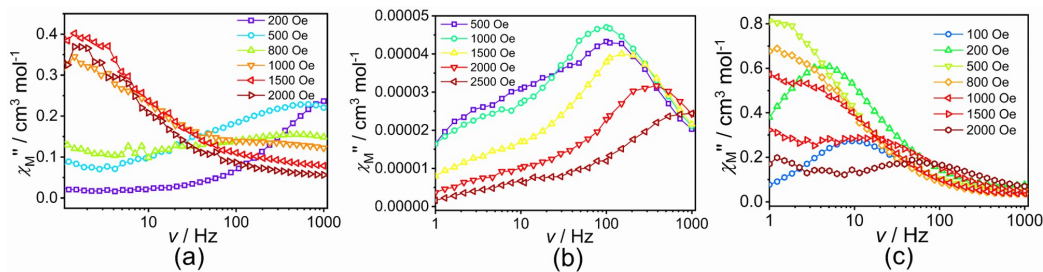


Fig. S7 Frequency dependence of χ_M'' susceptibilities for **1** (a), **2** (b) and **3** (c) under different dc fields.

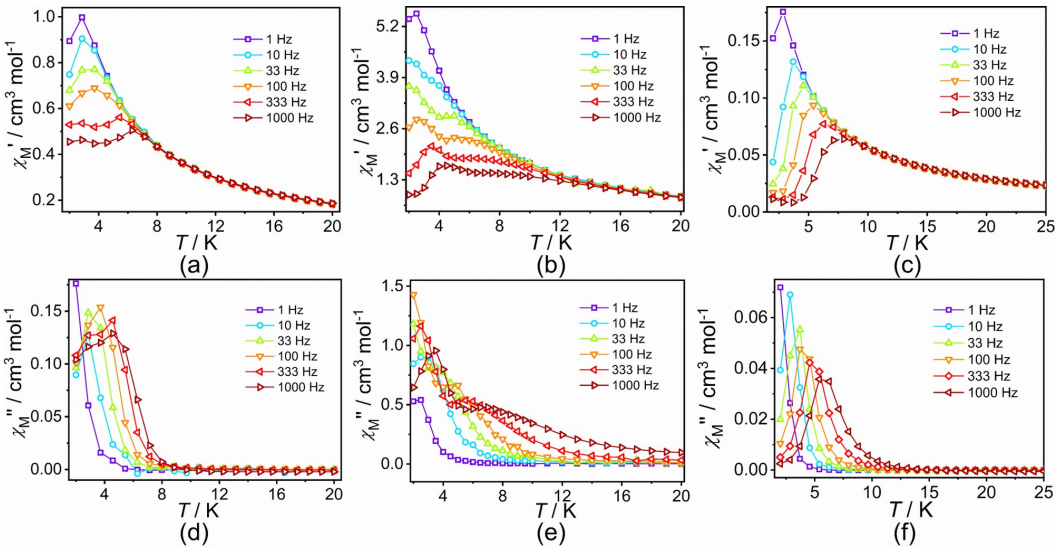


Fig. S8 Temperature dependence of the in-phase (χ'_M , top) and out-of-phase (χ''_M , bottom) ac susceptibilities at different frequencies under the external dc fields for complexes **1** (a, d), **2** (b, e) and **3** (c, f).

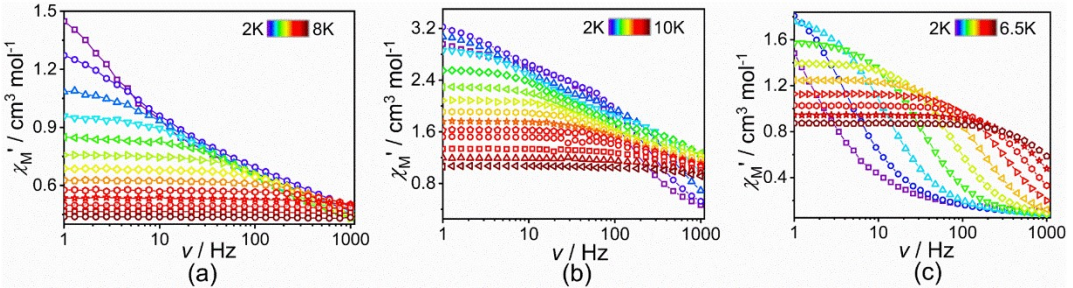


Fig. S9 Frequency dependence of χ'_M susceptibilities for **1** (a), **2** (b) and **3** (c) under the external dc fields.

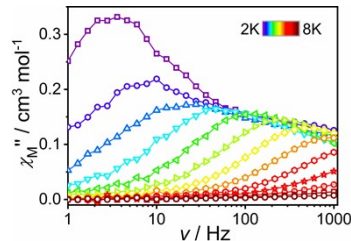


Fig. S10 Frequency dependence of χ''_M susceptibilities for **1** under the external dc fields.

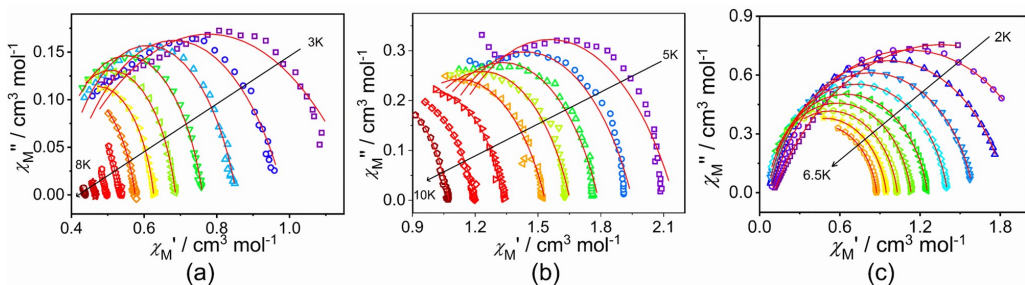


Fig. S11 Cole-Cole plots under the static dc fields for **1** (a), **2** (b) and **3** (c). The solid lines represent the best fit to the measured results.

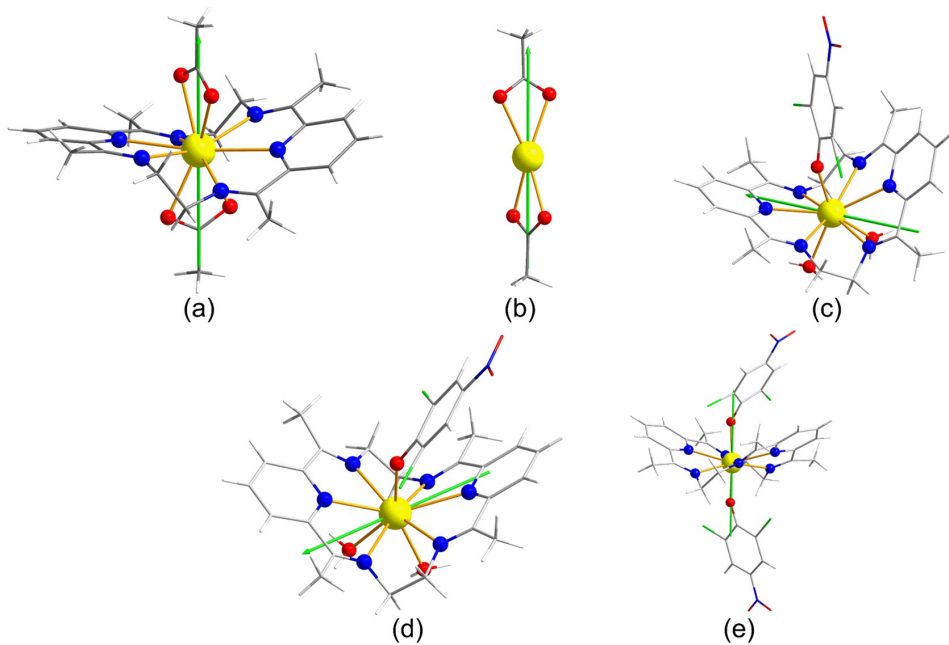


Fig. S12 Calculated orientations of the local main magnetic axes on Dy(III) in the ground KDs of **1** (a), **1a** (b), **2a** (c), **2b** (d) and **3** (e).

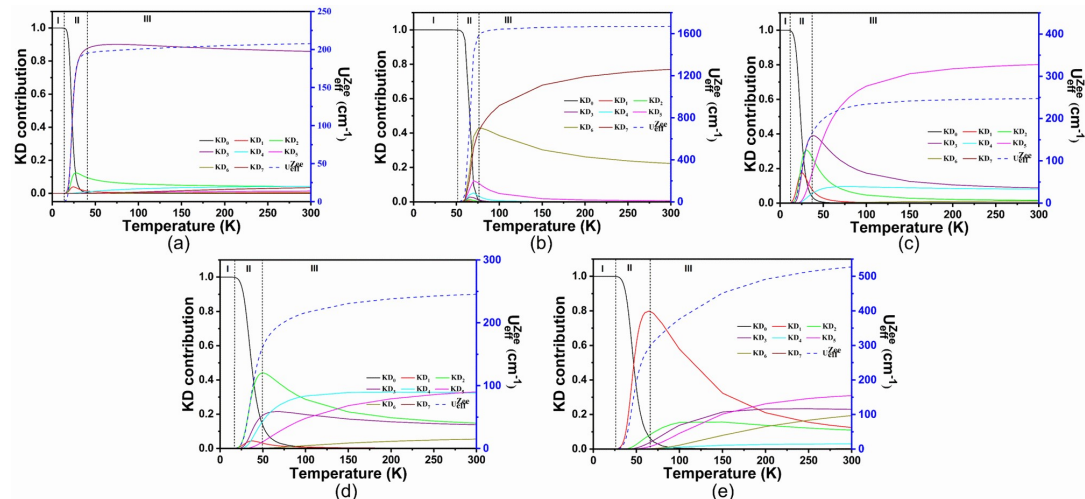


Fig. S13 Predicted effective barrier and relaxation contributions from various KDs of complexes **1** (a), **1a** (b), **2a** (c), **2b** (d) and **3** (e), U_{eff} is represented as a dashed black line, and its value is indicated on the right y-axis, the left y-axis represents the relative contribution of each KD to relaxation.